

M³Express: A Low-Cost Independently-Mobile Reconfigurable Modular Robot

Kevin C. Wolfe, Matthew S. Moses, Michael D.M. Kutzer, and Gregory S. Chirikjian

Abstract—This paper presents *M³Express* (Modular-Mobile-Multirobot), a new design for a low-cost modular robot. The robot is self-mobile, with three independently driven wheels that also serve as connectors. The new connectors can be automatically operated, and are based on stationary magnets coupled to mechanically actuated ferromagnetic yoke pieces. Extensive use is made of plastic castings, laser cut plastic sheets, and low-cost motors and electronic components. Modules interface with a host PC via Bluetooth® radio. An off-board camera, along with a set of modules and a control PC form a convenient, low-cost system for rapidly developing and testing control algorithms for modular reconfigurable robots. Experimental results demonstrate mechanical docking, connector strength, and accuracy of dead reckoning locomotion.

Index Terms—modular robots, self-reconfigurable systems, mechanism design for low-cost mobile robots

I. INTRODUCTION

Modular reconfigurable robots (MRRs) continue to experience remarkable development. Since the initial work in the 1990's [1]–[4], individual modules have become more capable, and increasing numbers of functional modules are being incorporated into working demonstrations [5]–[8]. However, the cost and complexity of most modular robot systems tends to increase almost as rapidly as their capabilities. Some counter-examples to the trend of increasing unit complexity include efforts in programmable matter [9] and swarm robotics [10]. However, in programmable matter the self-mobility of modules is not a central focus, and most (low-cost) swarm systems lack mechanical interconnectability.

The MRR presented here is intended as a low-cost testbed for real-world docking and reconfiguration algorithms; for demonstrations with large numbers of self-mobile, automatically-docking modules; and for classroom use in undergraduate engineering programs. A number of MRR projects have produced low-cost robots designed for education and broader public use. The most well-established of

This research was partially supported under an appointment to the Department of Homeland Security (DHS) Scholarship and Fellowship Program, administered by the Oak Ridge Institute for Science and Education (ORISE) through an interagency agreement between the U.S. Department of Energy (DOE) and DHS. ORISE is managed by Oak Ridge Associated Universities (ORAU) under DOE contract number DE-AC05-06OR23100.

This work was also supported in part by NSF grant IIS-0915542 RI: Small: Robotic Inspection, Diagnosis, and Repair.

K. Wolfe, M. Moses, M. Kutzer, and G. Chirikjian are with the Department of Mechanical Engineering, Johns Hopkins University, Baltimore, Maryland. {kevin.wolfe, matt.moses, mkutzer1, gregc}@jhu.edu

M. Moses and M. Kutzer are also with the Research and Exploratory Development Department, Johns Hopkins University Applied Physics Laboratory, Laurel, Maryland.

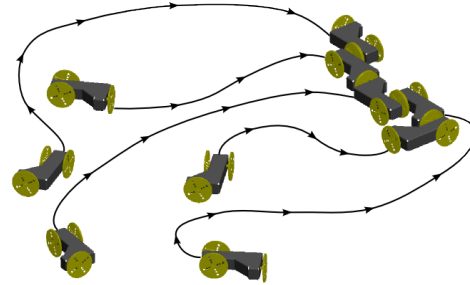


Fig. 1. Modules are independently mobile. Wheels function as interconnectors.

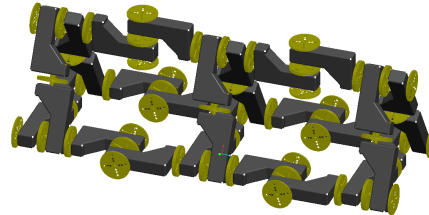


Fig. 2. Module geometry allows formation of complex chain and lattice structures. Here modules are shown in a triangular-prism lattice.

these is the open-source Moleculs project [11]. While made of components with relatively high availability, this design still relies on expensive components such as thin-section ball bearings and electrical slip-rings. Other examples of systems designed specifically for low cost and high availability are [12] and [13]. In all three of these cases, modules have a single degree of freedom and docking must be accomplished manually. In contrast, the new low-cost module presented in this paper has three independent degrees of freedom and three active mechanical connectors.

The robot presented here is morphologically similar to *M³*, the design initially presented in [14]. As in [14], the modules have three dual-purpose wheels which serve as driving wheels and mechanical inter-connectors (see Fig. 1). In some heterogeneous MRRs, special-purpose modules equipped with wheels are used to allow high mobility [15] or to quickly transport non-mobile modules [16]. A self-mobile module with four degrees-of-freedom and several new mobility modes was recently presented in [17], however this system does not currently have automatic connection ability. The *M³* is a homogeneous system with wheels and connectors combined into one dual-purpose mechanism. It is important to note that, the *M³* connectors will only mate when aligned in a discrete set of offset angles, which creates

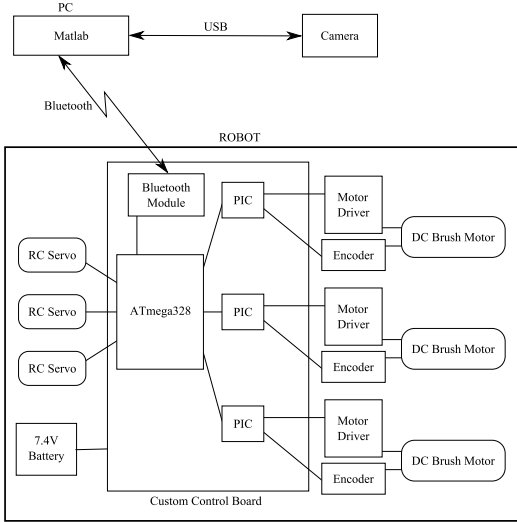


Fig. 3. Control Block diagram.

interesting challenges for planning and path generation. A path-planning algorithm for docking that accounts for this condition was presented in [18].

The initial motivation for the architecture of this modular system, as described in [14], is rapid damage repair/mitigation in hazardous environments. In a fully deployed system, the vision is that each module would serve as a section of “active conduit”, transmitting power and/or communications across adjacent connector faces. The design and geometric ratios of M^3 were chosen so that individual modules have a high degree of mobility and yet a group of modules are able to form a broad class of structures including chains and lattices (see Fig. 1 and Fig. 2). In particular, the M^3 system’s ability to form lattices allows cantilevers and towers to be built for crossing gaps and reaching elevated regions.

II. ARCHITECTURE

Modules of the M^3 system have three wheels, each of which serves as a connector. The dimensions of the wheel-to-wheel distances are chosen so that modules can form chains and lattices, as described in [14]. While the kinematics and overall geometric ratios of the present modules, M^3 Express, are similar to that of [14], there are several key differences that make M^3 Express easier to construct and faster to prototype. M^3 Express makes extensive use of plastic castings and laser-cut acrylic sheets. Low-cost off-the-shelf motors are chosen along with an on-board module control system that is stripped-down to the basic essentials of managing low-level motor control and relaying commands from a central PC. A single wheel connector uses two magnets affixed to the wheel, two spring-loaded mechanically actuated ferromagnetic “yokes”, and four locking pins. The “yokes” in this case are simply steel machine screws installed on pins such that they mate with complementary magnets in a mating wheel. Additionally, we introduce the use of an omniwheel on the perpendicular “third wheel” to aid in improving kinematic driving accuracy.

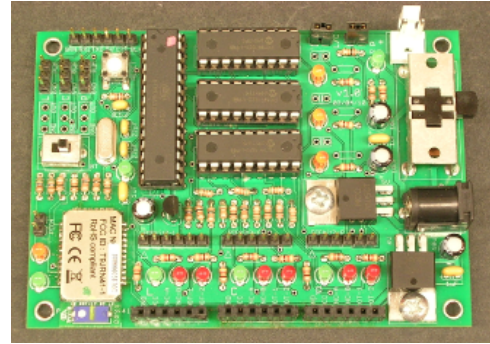


Fig. 4. The main components on the custom electronics board include an Atmel AVR for general I/O, three PIC microprocessors for low-level motor control, and a Bluetooth® module for wireless communication.

A. Control

To reduce cost, on board sensing is minimized through the use of external imaging. Multiple robots can operate in an arena observed by an overhead camera. A block diagram of the control for a single robot is shown in Fig. 3. The camera (Imaging Source P/N DFK 72BUC02) is used to find position, heading, and up-down orientation of each robot. The equations of motion for driving are different depending on whether a robot is “right-side up” or “upside down”—detecting this distinction is what is meant by up-down orientation. In this paper, only one orientation is used.

A real-time program running in MATLAB® interfaces to the camera over USB and to each robot in the arena via Bluetooth®. While the camera is currently offboard for simplicity, cameras could eventually be added onboard as in [19]. Before operation, the camera is registered to the scene by placement of four markers at known locations at each corner of the arena. Subsequent images are dewarped via the planar homography determined in the registration step. The camera captures an image approximately once per second. Fiducial markers on each robot are located via a multi-step corner-detecting filter. First, normalized cross-correlation is performed between the image and a rotationally symmetric template of concentric black-and-white circles. Then, corner detection is applied at the centers of locations of high cross-correlation. The detected corners are finally grouped and assigned to a particular module based on ratios of distances between the markers found. This process provides a fast, robust, and accurate method for tracking the modules.

Special absolute encoder markings on the perimeter of each wheel are used to provide a high-accuracy measurement of the wheel angles. While each wheel has its own relative encoder mounted on the pinion of the motor, the markings are helpful for several reasons: 1) the low-cost motors and gearboxes that drive the wheels have a high degree of backlash that is not measured by the encoder mounted close to the motor pinion; 2) the markings provide an absolute reference that can be used to initialize the state estimation on startup or reset; 3) the markings make state estimation more robust to non-catastrophic hardware failure such as encoder drift; 4) data bandwidth between module and computer is

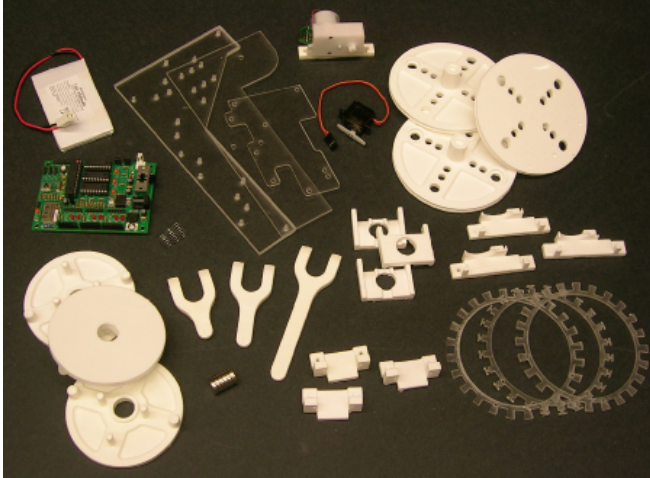


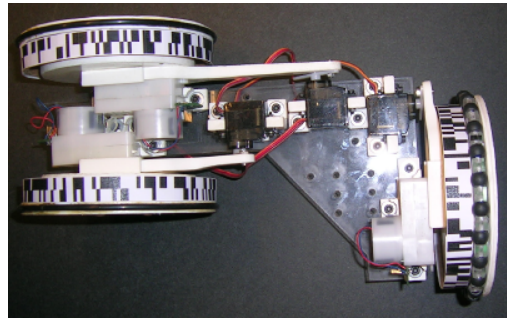
Fig. 5. Modules are built of low-cost easily available motors, and quickly fabricated plastic components.

reduced as position, orientation, and wheel angles can all be simultaneously captured by the camera.

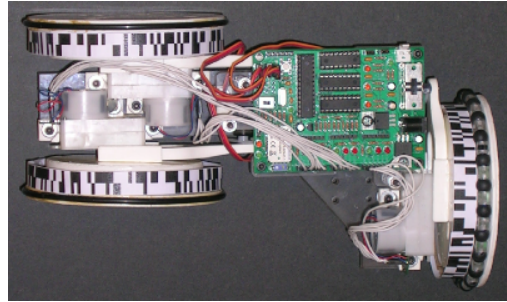
Once the configuration is obtained, a planning routine determines the motion commands to send to the robot. A string of serial commands is sent over Bluetooth®, and the serial commands are received and processed by the onboard processor. The processor is an Atmel ATmega328 running Arduino firmware [20]. Serial commands are parsed, and then motion commands are sent to three PIC18F1320 microprocessors with a Step/Direction interface. Each PIC performs closed loop position and/or speed control on the motors, counts encoder pulses, and outputs a PWM signal to the motor driver. The motor drivers (Solarbotics P/N 51510) are installed aftermarket on the off-the-shelf DC motors. The Arduino can report a status packet back to the PC, however this is currently not used.

B. Construction

The module has a plastic laser cut chassis that holds three brushed DC motors (Solarbotics P/N GM17) and three miniature RC servo motors (see Fig. 6). To these motors and servos, the wheels and docking mechanisms are attached using mounting brackets (see Fig. 7). The wheels, docking mechanisms, motor mounts and servo mounts are made of polyurethane that was cast in silicone molds. Masters for these molds were created using a 3D printer. The reusable silicone molds allow parts to be produced quickly and economically with little post-processing. The two primary drive wheels are fitted with large diameter rubber o-rings which act as tires. The third perpendicular wheel is fitted with a custom omni-directional wheel (omniwheel) whose construction is described in Section II-D. In addition to mechanical components, a custom electronics board and 7.4 V lithium polymer battery pack are attached to the frame. Lastly, fiducial markers are applied to the module to allow for tracking using an overhead camera.



(a) Chassis with motors, servos, and wheels.



(b) Module with electronics.

Fig. 6. Above is an overview of how the module is constructed.

C. Interconnect Mechanism

The interconnect mechanism is similar to the spring-loaded magnet system presented in [21]. The interconnect in [21] is actuated by shape-memory alloy, while our mechanism is actuated by a miniature RC servo driving a sliding wedge mechanism (see Fig. 7). The sliding wedge mechanism functions as a mechanical slip ring. A section view of two mating connectors is shown in Fig. 8. The connectors are genderless, but they must be offset by 90° or 270° in order to mate. In each wheel, two magnets are statically mounted. A smaller sliding disk carries two steel screws and four tapered pins, all of which insert through holes in the wheel. Springs between the wheel and sliding disk push them apart. The springs are strong enough to overcome the magnetic attraction force when two wheels are mated. The motor-driven wedge overcomes the spring force to push the sliding disk outward and engage the connectors. This design allows strong magnetic attraction to be turned on and off by a small motor. In addition, the servo motor only operates when the connector is changing state and does not need to run continuously.

In contrast to most other MRR designs, our system currently does not have a means for hard-wired intermodule communication (although the Bluetooth® radios can be used for wireless linking). There is ample space on the wheel where off-the-shelf spring-loaded electrical contacts could be installed, but the cabling to these contacts would either limit the free rotation of the wheel or necessitate an electrical slip ring. While slip rings are often used in MRRs [11], [14], they are not the best choice in a design focused, high availability, ease of manufacturing, and low-cost parts.

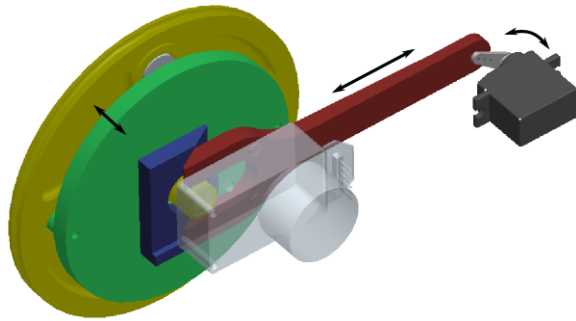


Fig. 7. The mechanical interconnection mechanism is driven by a sliding wedge connected to a miniature RC servo.

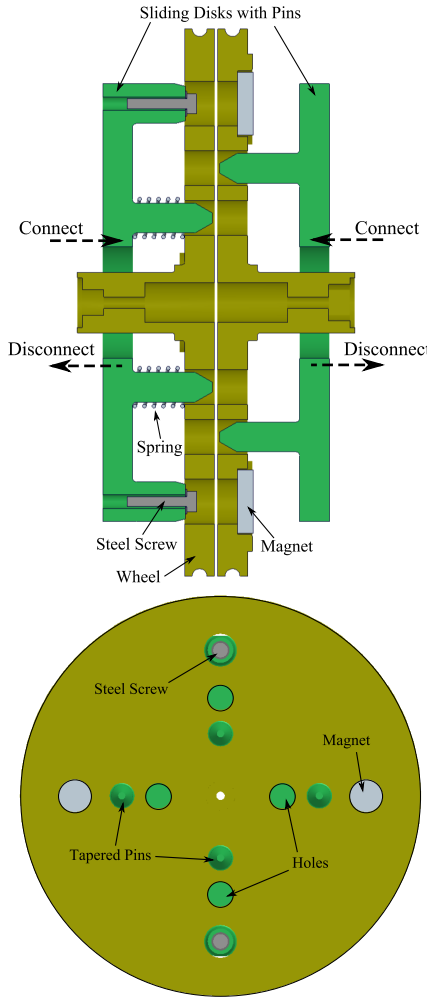


Fig. 8. Section view of two mating wheels (top). View of the wheel face (bottom). Dashed arrows indicate motion of the components for connection and disconnection.

A design for an optical communication port allowing for free rotation of the wheel is shown in Fig. 9. A ring-shaped diffuser made of translucent plastic is embedded in the perimeter of each wheel. This forms a diffuse window that allows visibility of an emitter and detector mounted statically to the robot chassis. When two robots are mated, the arrangement provides a half-duplex communication channel.

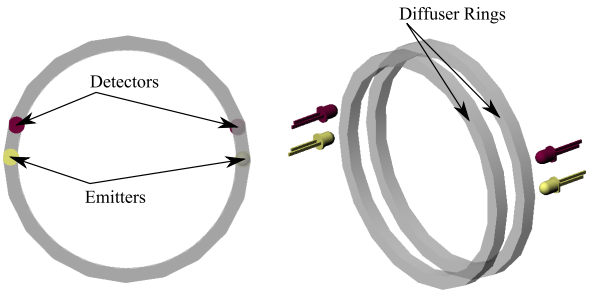


Fig. 9. Conceptual design showing a mating pair of optical interconnects. An emitter/detector pair is mounted statically to the frame and a ring-shaped diffuser is embedded in each wheel.

During transmission, light from the emitter on one robot will illuminate the entire diffuser ring. This light can then be picked up by the detector on the other robot, independent of wheel rotation angle. Multiple emitters can be used if stronger illumination is needed. This design should provide a low-cost non-contact high bandwidth serial communication channel for each mated connector; implementation is an area for future work.

D. Omni-directional Wheel (Omniwheel)

As discussed in [14] and [18], the “third wheel” of the robot is mounted orthogonally to the driving wheels so that multiple robots can form complex three-dimensional structures. However, the design and weighting of each module still allows it drive in plane as a differential-drive robot (also commonly known as the classic kinematic cart). The addition of the third wheel does cause some issues; the friction experienced by the perpendicular wheel increases slipping and scuffing of the two drive wheels. While the original system in [14] did not explicitly address this issue, two proposed strategies for reducing this friction were considered for *M³Express*: the addition of ball casters near the third wheel to lift it off the ground, and the use of an omniwheel. After testing both approaches, the omniwheel was chosen. This choice was made because it allowed a module to track the kinematic model presented in Section III much more accurately, especially during commonly used trajectories—straight driving and pivots. During straight-ahead travel, the omniwheel is very effective at reducing the frictional drag experienced. However, during pivots, the omniwheel is used to effectively increase the traction of the module.

The omniwheel is constructed by adding a ring of rollers to the perimeter of the existing third wheel. The rollers are made of hobby beads with “tires” made of heatshrink tubing. Roller axles are made of stiff steel wire. The rollers and axles are then sandwiched between three layers of 1.5 mm lasercut plastic, which is then mounted to the wheel casting.

III. KINEMATICS AND CONTROLLABILITY

As previously described, the modules can be driven and steered like a differential-drive robot. However for two modules to dock, the position and orientation of the modules must be compatible, along with the orientation of their adjacent

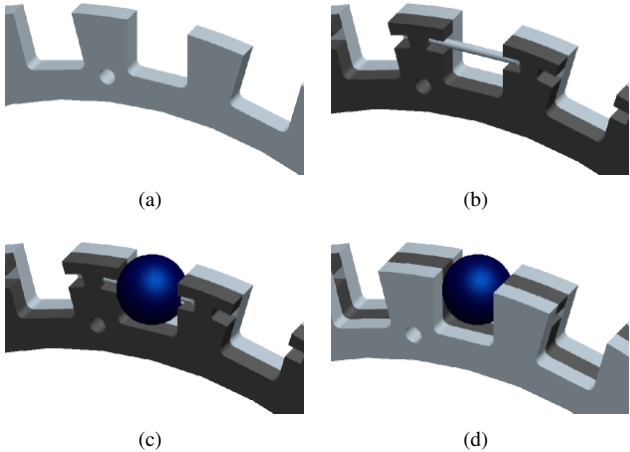


Fig. 10. The omniwheel is built of a ring of rollers, with roller axles captured by three laser-cut disks.

wheels. Thus, in addition to x , y , and θ , the angles of the wheels (i.e., ϕ_C , ϕ_L , and ϕ_P) are also considered. When the pose (x, y, θ) of a single module is defined as shown in Fig. 11, the kinematic equations of motion are given by

$$\dot{\mathbf{x}}(t) = G \begin{pmatrix} \dot{\phi}_C \\ \dot{\phi}_L \end{pmatrix} \quad (1)$$

for

$$\dot{\mathbf{x}}(t) = \begin{pmatrix} \dot{x} \\ \dot{y} \\ \dot{\theta} \\ \dot{\phi}_C \\ \dot{\phi}_L \end{pmatrix} \text{ and } G = \frac{r}{2} \begin{pmatrix} -\sin(\theta) & \sin(\theta) \\ \cos(\theta) & -\cos(\theta) \\ -\frac{2}{W} & -\frac{2}{W} \\ \frac{r}{2} & 0 \\ 0 & \frac{2}{r} \end{pmatrix}$$

where $\dot{\phi}_C$ and $\dot{\phi}_L$ are driving wheel velocities defined as shown in Fig. 11. This model assumes a no-slip condition for the two drive wheels.

The friction experienced by the third perpendicular wheel can cause this assumption to be violated. As described in Section II-D, we added an omniwheel to this third wheel to help the module track (1) more accurately. The velocity of the omniwheel is determined using a slip-minimizing condition for the third wheel [14], [18]. As a function of the velocities of the two drive wheels, this slip-minimizing constraint is given as

$$\begin{aligned} \dot{\phi}_P &= \frac{-L}{r} \dot{\theta} \\ &= \frac{L}{W} (\dot{\phi}_C + \dot{\phi}_L) \\ &= 2 (\dot{\phi}_C + \dot{\phi}_L). \end{aligned} \quad (2)$$

When considering control strategies for docking two modules, it is important to note that the system in (1) is not controllable due to a holonomic constraint between θ , ϕ_C , and ϕ_L . However, if we consider a system $\mathbf{x}_C(t) = (x, y, \theta, \phi_C)^T$ it can be shown that the new system is small-time locally controllable. This can be demonstrated by performing two Lie bracket operations as defined in [22].

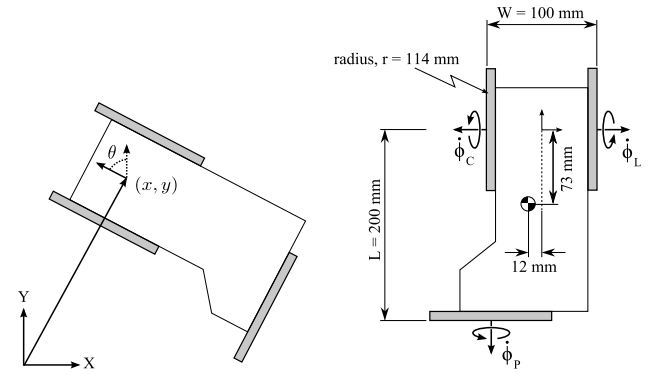


Fig. 11. (Left) The pose of a module can be represented using x , y , and θ as shown. (Right) Relevant module dimensions for kinematic driving and reference directions for rotation of each of the three wheels. The center of mass is also shown.

Letting $r = W = 1$, we can relate \mathbf{g}_1 and \mathbf{g}_2 to the columns of G such that

$$\dot{\mathbf{x}}_C(t) = \mathbf{g}_1 \dot{\phi}_C + \mathbf{g}_2 \dot{\phi}_L$$

where

$$\mathbf{g}_1 = \begin{pmatrix} -\frac{\sin(\theta)}{\cos^2(\theta)} \\ \frac{2}{\cos(\theta)} \\ -1 \\ 1 \end{pmatrix} \text{ and } \mathbf{g}_2 = \begin{pmatrix} \frac{\sin(\theta)}{2} \\ -\frac{2}{\cos(\theta)} \\ -1 \\ 0 \end{pmatrix}.$$

It can then be shown that

$$[\mathbf{g}_1, \mathbf{g}_2] = \begin{pmatrix} -\cos(\theta) \\ -\sin(\theta) \\ 0 \\ 0 \end{pmatrix}$$

and

$$[\mathbf{g}_1, [\mathbf{g}_1, \mathbf{g}_2]] = \begin{pmatrix} -\sin(\theta) \\ \cos(\theta) \\ 0 \\ 0 \end{pmatrix}.$$

It is clear that these four vectors are linearly independent and thus the reduced system is small-time locally controllable. This can be similarly shown for a reduced system of x , y , θ , and ϕ_L .

Note that, if we look at a system of x , y , θ , and ϕ_P with respect to (1) and (2), this system is not controllable. However, since the perpendicular wheel is intended to slip to some degree, this can be overcome for docking by intentionally slipping this wheel once the proper pose is realized. This strategy has proven to be successful in experimental testing.

IV. PERFORMANCE

A testbed system was implemented, including a fully-functional robot, a lightweight non-functional dummy module, an overhead camera with associated PC, and MATLAB® control software. Some simple docking tests were performed and various robot capabilities were measured.

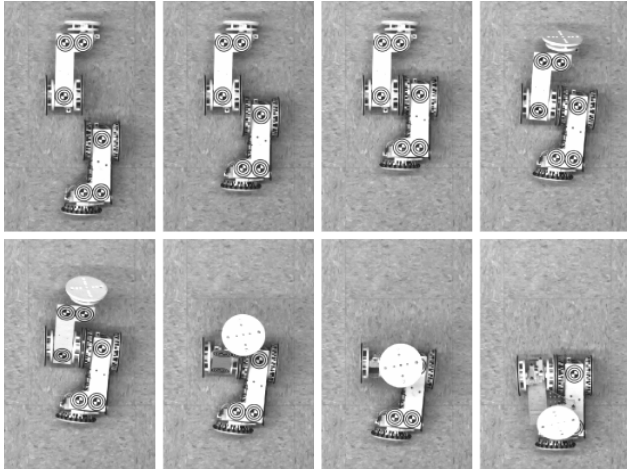


Fig. 12. Sequence proceeds left to right, top to bottom. A fully-functional module approaches a dummy docking target, connects, and then lifts the newly connected dummy module.

TABLE I
COSTS AND MASSES FOR A SINGLE *M³ Express* MODULE

Item	Cost	Mass
polyurethane castings	\$4	344 g
laser cut acrylic components	\$18	152 g
3 × DC gearmotors	\$17	105 g
3 × DC motor drivers/encoders	\$30	15 g
3 × RC servos	\$12	32 g
main circuit board	\$73	57 g
LiPo battery (7.4 V 1500 mAH)	\$21	66 g
6 × magnets	\$6	18 g
cables and hardware	\$9	89 g
Total	\$190	878 g

A. Cost

One goal of this design was to make a module that was inexpensive, so that modules could be produced in significant numbers. Table I provides an overview of the cost associated with a single module. Cost estimates for many modular robots are not widely published; however, several low-cost systems do exist including GZ-I (an updated version of Y1 with a cost less than \$280) [13], DoF-Box (\$120) [12], and Molecubes (\$242 without electronics) [11]. With a total cost of around \$190 per module, the new *M³ Express* module is of similar expense to those reported previously. This cost estimate does not include labor. Still, given the design and fabrication techniques utilized, small batch production should allow modules to be produced at a rate of approximately one per three to four hours. Its cost is also less than one tenth the cost of the original *M³* module presented in [14].

B. Weight and Torque

Each module has a mass of 878 g. Table I provides a breakdown of masses of various components. The center-of-mass of the module was found by measuring the wheel weight distribution, and is shown in Fig. 11. This, combined with the weight of the module, determines the required torque for a module to lift itself out of plane along its long axis (similar to what is shown in Fig. 12). This torque was calculated to be 0.63 N·m. However, the motors produce an effective stall torque of 0.32 N·m at the wheel face. Thus, at

present the module is unable to lift itself or another module. Strategies for overcoming this are discussed in Section V.

C. Docking Experiments

The docking mechanism was tested by manually aligning a lightweight (494 g) non-functional module near a fully-functional module. The functional module was then remotely commanded to drive next to the target, extend its pin plate, and lift the dummy module. This process was remotely controlled by a human operator sending commands via the MATLAB® interface. Successful docking and lifting was achieved, showing that the docking mechanism works as designed and the docking process is viable. Fig. 12 presents a sequence of images captured by the overhead camera during the test.

In addition to testing whether the docking mechanism was able to connect two modules, the strength of the connection was tested. When axially loaded at the center of the two docked wheels, the docking mechanisms provide a holding force of 11 N (the module itself weighs 8.6 N). When the axial load is applied at the rim of the wheel, the holding force is reduced to 4.8–5.5 N and is dependent on the exact location of loading. In shear, the holding force is much higher; it is effectively limited by the shear strength of the locking pins.

D. Driving, Slip, and Scuffing

The module, as currently configured in software, has a maximum driving speed of 3.1 cm/s. The speed of the module was capped to help prevent slip of the drive wheels. Despite attempts to minimize slip (e.g., increasing tire friction and introduction of the omniwheel), the module experiences a nontrivial amount of slip. This slip and scuffing lead to deviation from the expected kinematic driving behavior described in Section III and [18]. Fig. 13 shows the superposition of the final module locations from 25 trials of commanding the robot to drive forward 500 mm in an open-loop fashion. The results indicate that, for trajectories of significant length, a closed-loop control law will need to be coupled with the results from [18] to achieve repeatable docking of modules with arbitrary initial positioning.

V. CONCLUSIONS AND FUTURE WORK

A new “Express” design for the modules of the *M³* system was designed and prototyped. The module was designed to be easily assembled, and incorporates primarily off-the-shelf or easy to manufacture components, making it low-cost. The design and architecture produce a modular system that is potentially useful for educational outreach and/or use in an undergraduate setting. While the modules do not perform as well as those described in [14], they are useful for rapidly testing real-world control algorithms on a group of several robots at less than one tenth the cost. For example, since the modules are independently mobile and able to dock with one another in the plane, reconfiguration strategies can be investigated for three-dimensional structures that can be “unfolded” and initially formed in the plane such as the truss in Fig. 2.

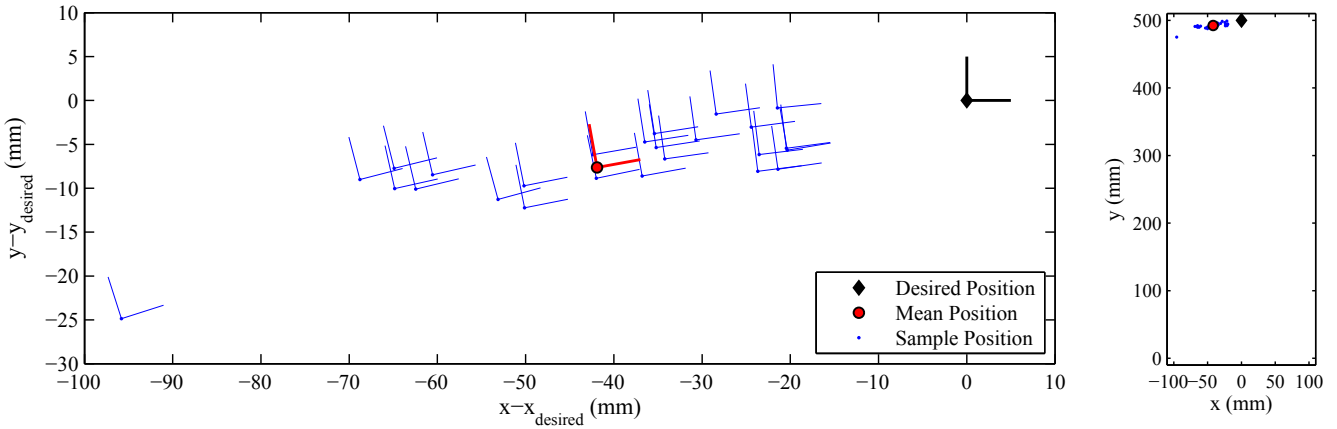


Fig. 13. Fiducial locations from ten trials of running the robot straight ahead from a known initial starting place. A closeup of error in final location is shown on the left, while absolute position is shown to scale on the right.

During testing, several things were discovered that can be improved. The module cannot lift itself or additional docked modules. There are several ways to address this issue: 1) the weight of the robot can be reduced by adding lightweight filler material to the polyurethane castings, 2) unnecessary material can be removed from the laser-cut parts, and 3) the overall size of the module can be reduced. Improving the output torque can be achieved by: 1) selecting new motors, 2) reducing friction in the drivetrain, and 3) applying a higher voltage across the motors through the use of a second 11.1 V lithium polymer battery pack. Another future improvement could include the creation of a single molded frame that would incorporate the servo and motor mounts. This would also make the module cheaper and easier to manufacture.

Future goals include building and testing additional modules, developing closed-loop control strategies for autonomous docking of modules, and investigating planning methods for 3D docking and assembly.

REFERENCES

- [1] T. Fukuda and S. Nakagawa, "Approach to the dynamically reconfigurable robotic system," *Journal of Intelligent & Robotic Systems*, vol. 1, pp. 55–72, 1988.
- [2] S. Murata, H. Kurokawa, and S. Kokaji, "Self-assembling machine," in *Proceedings of the IEEE International Conference on Robotics and Automation*, 1994, pp. 441–448.
- [3] M. Yim, "Locomotion with a unit-modular reconfigurable robot," Stanford University, Tech. Rep., 1994.
- [4] G. Chirikjian, "Kinematics of a metamorphic robotic system," in *Robotics and Automation, 1994. Proceedings., 1994 IEEE International Conference on*, May 1994, pp. 449 –455 vol.1.
- [5] K. Stoy, R. Nagpal, and W.-M. Shen, Eds., *Modular Robots: The State of the Art, Proceedings of the IEEE 2010 International Conference on Robotics and Automation Workshop*. IEEE, 2010.
- [6] M. Yim, W.-M. Shen, B. Salemi, D. Rus, M. Moll, H. Lipson, E. Klavins, and G. Chirikjian, "Modular self-reconfigurable robot systems [Grand Challenges of Robotics]," *IEEE Robotics & Automation Magazine*, vol. 14, no. 1, pp. 43–52, Mar. 2007.
- [7] S. Murata and H. Kurokawa, "Self-reconfigurable robots: Shape-changing cellular robots can exceed conventional robot flexibility," *IEEE Robotics & Automation Magazine*, pp. 71–78, Mar. 2007.
- [8] R. Groß, M. Bonani, F. Mondada, and M. Dorigo, "Autonomous self-assembly in swarm-bots," *IEEE Trans. Robotics*, vol. 22, no. 6, pp. 1115–1130, Dec. 2006.
- [9] K. Gilpin, A. Knaian, and D. Rus, "Robot pebbles: One centimeter modules for programmable matter through self-disassembly," in *Robotics and Automation (ICRA), 2010 IEEE International Conference on*, May 2010, pp. 2485 –2492.
- [10] M. Rubenstein and R. Nagpal, "Kilobot: A robotic module for demonstrating behaviors in a large scale (2^{10} units) collective," in *Proceedings of the IEEE 2010 Int. Conf. on Robotics and Automation workshop "Modular Robots: The State of the Art"*, 2010, pp. 53–57.
- [11] V. Zykov, A. Chan, and H. Lipson, "Molecubes: An open-source modular robotics kit," in *IROS-2007 Self-Reconfigurable Robotics Workshop*, 2007. [Online]. Available: <http://www.molecubes.org/>
- [12] D. Daidie, O. Barbey, A. Guignard, D. Roussy, F. Guenter, A. Ijspeert, and A. Billard, "The DoF-box project: An educational kit for configurable robots," in *Advanced Intelligent Mechatronics, 2007 IEEE/ASME International Conference on*, September 2007, pp. 1–6.
- [13] H. Zhang, J. Gonzalez-Gomez, Z. Xie, S. Cheng, and J. Zhang, "Development of a low-cost flexible modular robot GZ-I," in *Proceedings of the 2008 IEEE/ASME International Conference on Advanced Intelligent Mechatronics*, 2008.
- [14] M. D. M. Kutzer, M. S. Moses, C. Y. Brown, D. H. Scheidt, G. S. Chirikjian, and M. Armand, "Design of a new independently-mobile reconfigurable modular robot," in *Proc. IEEE International Conf. on Robotics and Automation*, May 2010.
- [15] F. Hou, N. Ranasinghe, B. Salemi, and W.-M. Shen, "Wheeled locomotion for payload carrying with modular robot," in *Intelligent Robots and Systems, 2008. (IROS 2008). 2008 IEEE/RSJ International Conference on*, Sept. 2008, pp. 1331–1337.
- [16] S. Kernbach, O. Scholz, K. Harada, S. Popesku, J. Liedke, H. Raja, W. Liu, F. Caparrelli, J. Jemai, J. Havlik, E. Meister, and P. Levi, "Multi-robot organisms: State of the art," in *ICRA 2010 Workshop - Modular Robotics: State of the Art*, 2010.
- [17] G. Ryland and H. Cheng, "Design of iMobot, an intelligent reconfigurable mobile robot with novel locomotion," in *Robotics and Automation (ICRA), 2010 IEEE International Conference on*, May 2010, pp. 60 –65.
- [18] K. C. Wolfe, M. D. Kutzer, M. Armand, and G. S. Chirikjian, "Trajectory generation and steering optimization for self-assembly of a modular robotic system," in *Proc. IEEE International Conf. on Robotics and Automation*, May 2010.
- [19] B. Shirmohammadi, M. Yim, J. Sastra, M. Park, and C. Taylor, "Using smart cameras to localize self-assembling modular robots," in *Distributed Smart Cameras, 2007. ICDS'07. First ACM/IEEE International Conference on*, Sep 2007, pp. 76 –80.
- [20] "Arduino - homepage," <http://arduino.cc/>.
- [21] S. Murata, E. Yoshida, K. Tomita, H. Kurokawa, A. Kamimura, and S. Kokaji, "Hardware design of modular robotic system," in *Proceedings of the 2000 IEEE/RSJ International Conference on Intelligent Robots and Systems*, 2000, pp. 2210–2217.
- [22] R. M. Murray, Z. Li, and S. S. Sastry, *A Mathematical Introduction to Robotic Manipulation*. CRC Press, 1994.